**Article:**
Rupani, M., Cleland, L.D. and Saal, H.P. (2025) Local postural changes elicit extensive and diverse skin stretch around joints, on the trunk and the face. Journal of The Royal Society Interface, 22 (223). 20240794. ISSN: 1742-5689

https://doi.org/10.1098/rsif.2024.0794

INTERFACE

royalsocietypublishing.org/journal/rsif



Research

**Cite this article:** Rupani M, Cleland LD, Saal HP. 2025 Local postural changes elicit extensive and diverse skin stretch around joints, on the trunk and the face. *J. R. Soc. Interface* **22**: 20240794.
https://doi.org/10.1098/rsif.2024.0794

Received: 6 November 2024
Accepted: 21 January 2025

**Subject Category:**
Life Sciences–Engineering interface

**Subject Areas:**
biomechanics

**Keywords:**
skin mechanics, proprioception, mechanoreception, body posture

**Author for correspondence:**
Hannes P. Saal
e-mail: h.saal@sheffield.ac.uk



# Local postural changes elicit extensive and diverse skin stretch around joints, on the trunk and the face

Mia Rupani[1], Luke D. Cleland[1,2] and Hannes P. Saal[1,2]

[1]Active Touch Laboratory, School of Psychology, University of Sheffield, Sheffield, UK
[2]Insigneo Institute for in silico Medicine, University of Sheffield, Sheffield, UK

LDC, 0000-0001-8486-2780; HPS, 0000-0002-7544-0196

Skin stretch, induced by bodily movements, offers a potential source of information about the conformation of the body that can be transmitted to the brain via stretch-sensitive mechanoreceptive neurons. While previous studies have primarily focused on skin stretch directly at joints, here we investigate the extent and complexity of natural skin stretch across various body regions, including the face and trunk. We used a quad-camera set-up to image large ink-based speckle patterns stamped on participants' skin and calculated the resulting stretch patterns on a millimetre scale during a range of natural poses. We observed that skin stretch associated with joint movement extends far beyond the joint itself, with knee flexion inducing stretch on the upper thigh. Large and uniform stretch patterns were found across the trunk, covering considerable portions of the skin. The face exhibited highly complex and non-uniform stretch patterns, potentially contributing to our capacity to control fine facial movements in the absence of traditional proprioceptors. Importantly, all regions demonstrated skin stretch in excess of mechanoreceptive thresholds, suggesting that behaviourally relevant skin stretch can occur anywhere on the body. These signals might provide the brain with valuable information about body state and conformation, potentially supplementing or even surpassing the capabilities of traditional proprioception.

## 1. Introduction

The human sense of touch plays a critical role in our interaction with the environment and in learning about our own bodies. Skin stretch, a fundamental component of touch, provides us with rich sensory information about both of these aspects. When we contact an object, even a slight slip [1] can trigger a surge of neural activity [2]. Perceptually, we are also exquisitely sensitive to stretch when applied to the skin passively [3]. Beyond external stimuli, skin stretch also contributes to proprioception, our sense of body position and movement. As we flex our joints, such as the fingers or knees, the resulting skin deformation provides valuable cues that complement the signals from traditional proprioceptors [4–8]. Indeed, some mechanoreceptors are highly sensitive to skin stretch elicited by joint movements, responding to stretch that causes the skin to elongate by as little as 1% [9].

While the role of skin stretch in joint movement has been explored, a critical question remains: how far does this influence extend beyond the immediate vicinity of joints? Moreover, how does skin stretch operate in regions with more complex underlying anatomy, such as the trunk or the face? In the face, specifically, lacking traditional proprioceptors [10], skin stretch has been proposed as a potential source of information for facial proprioception [11,12]. However, the complex nature of facial movements compared to simpler hinge joints necessitates a deeper understanding of the



THE ROYAL SOCIETY PUBLISHING

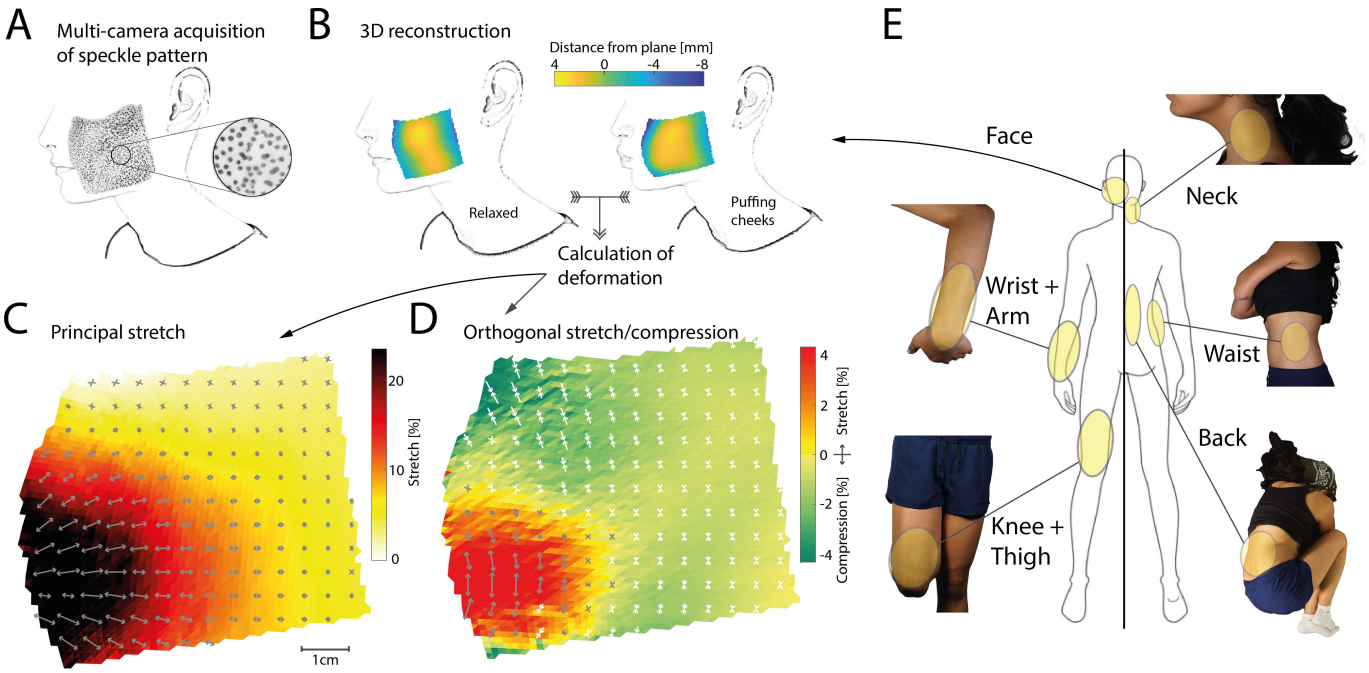


**Figure 1.** Data acquisition framework and targeted body regions. (A) An ink-based random dot speckle pattern was applied to the targeted skin region and imaged through up to four high-resolution cameras simultaneously. The example shown here is a roughly 8 × 8 cm patch applied to the cheek of a participant. Individual speckle dots are clearly visible in the inset. The original photograph has been digitally converted to outlines with some features removed. (B) Local speckle patterns are correlated across two or more cameras using digital image correlation to obtain a three-dimensional reconstruction of the imaged skin surface patch. In the examples shown, a two-dimensional plane has been fit to the reconstructed three-dimensional surface, with colours denoting the distance of each local patch from that plane, illustrating the shape of the cheek area. Left: A relaxed pose, serving as the baseline for stretch calculations. Right: The participant is puffing their cheeks, which results in a bulging of the cheek area close to the mouth in the three-dimensional reconstruction. Considering both reconstructions together allows calculation of skin deformation from the baseline relaxed pose. (C) Magnitude (coloured shading) and direction (arrows) of the principal stretch, i.e. the stretch along the direction in which it is largest, when the participant is puffing their cheeks. Darker shading indicates larger stretch which reaches upwards of 25% close to the mouth. Arrows indicate the direction of stretch, which is not uniform across the imaged area. All measures are shown projected onto the best-fitting plane, with stretch magnitudes subsampled to 1 mm and directions subsampled to 5 mm resolution for better visibility. (D) Magnitude and direction of stretch in the direction orthogonal to the principal direction (as shown in C). Yellow/red shading indicates positive stretch, implying that in these regions the skin expands in all directions. Green shading and white arrows indicate compression. Note the generally smaller stretch magnitudes along this secondary axis. (E) Body regions where stretch values were measured. These include the face, the wrist/arm and knee/thigh regions, as well as the neck, waist and back.

stretch signal. Existing research on skin stretch has often relied on simplified, one-dimensional measurements of stretch along a specified axis, failing to capture the full complexity of the stretch signal. As the body undergoes three-dimensional conformational changes, the skin, which envelops it, stretches and compresses in two dimensions on its surface. This spatial complexity raises questions about the signals available to the brain and how they might be interpreted to estimate body configuration.

To address these limitations, this study employs a high-resolution measurement approach to map skin stretch across various body regions during static postures. By quantifying the extent and characteristics of skin stretch, we aim to further elucidate its potential role in proprioception and, more generally, the perception of local skin conformation. The findings will lay the groundwork for further research into how the brain integrates and utilizes skin stretch information to arrive at a rich and nuanced understanding of our body in the world.

## 2. Results

We developed a multi-camera set-up for gathering high-resolution simultaneous images of random speckle ink patterns applied to the skin across large patches (figure 1A, refer to Methods (§4) for details). Correlating the local speckle patterns across multiple cameras allowed us to automatically reconstruct the three-dimensional surface and characterize the shape of complex skin deformation under different poses (figure 1B). From these measures, we calculated the principal stretch magnitudes and their directions (refer to Methods (§4)) at a resolution of around 1 $mm^2$, yielding detailed stretch maps across the full patch (figure 1C). We also characterized how the skin deformed in the direction orthogonal to the principal stretch, where it could also stretch or sometimes compress (figure 1D). Using this general processing pipeline, we measured stretch induced by different body postures at a variety of skin regions, such as at and around joints, on the trunk, as well as on the face (figure 1E) for patches up to 369 $cm^2$ in size across 15 participants.

### 2.1. Large spatial extent of skin stretch around joints

First, we investigated skin stretch around joints where it has been implicated in proprioception. Prior work had reported that putative stretch-sensitive mechanoreceptors on the upper thigh responded to even slight knee flexion [13], indicating that skin

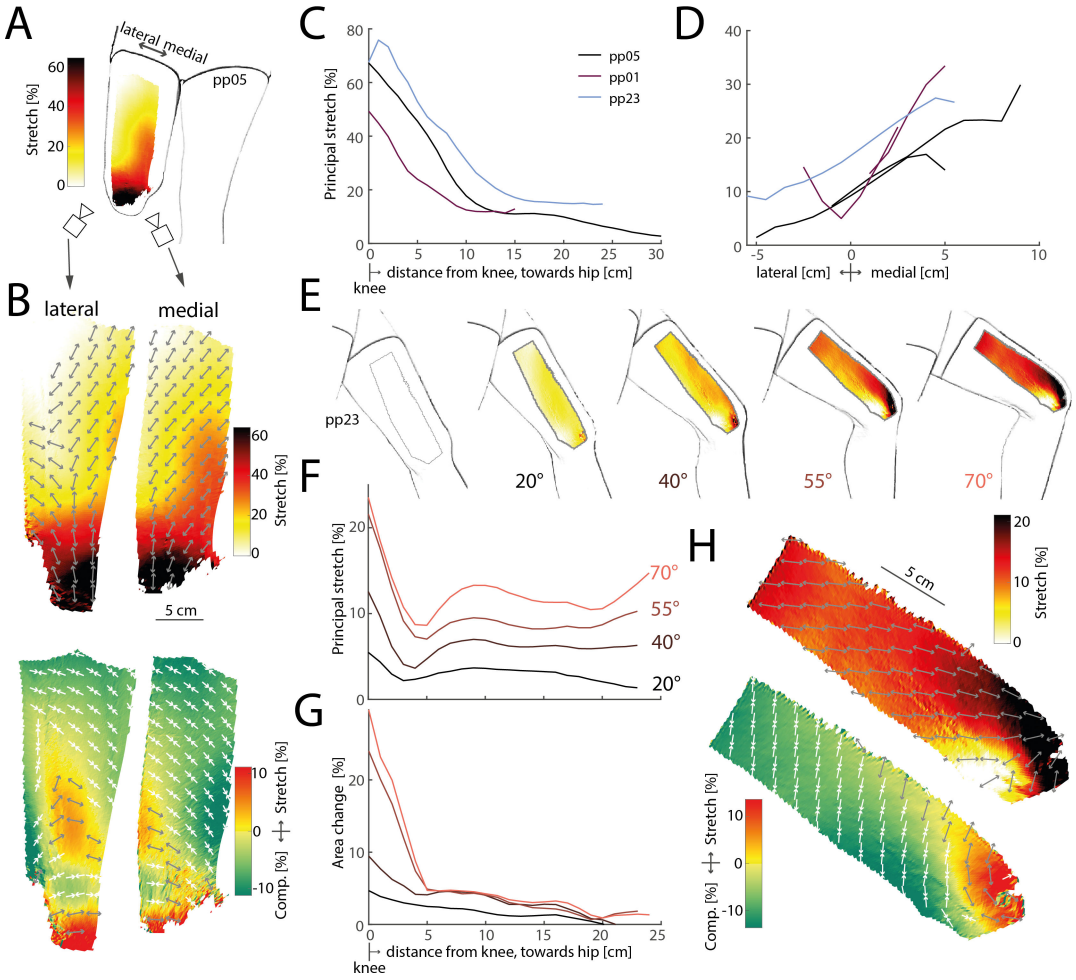


**Figure 2.** Stretch patterns on knee and thigh skin in response to flexion of the knee. (A) Principal stretch on the thigh under maximal flexion of the knee. Stretch reaches more than 60% at the knee, but is still around 20% on the upper thigh. (B) Detailed maps of principal (top row) and orthogonal (bottom row) stretch on the lateral (left column) and medial (right column) thigh. (C) Average principal stretch from distal (knee) to proximal (upper thigh) for three participants. Stretch is highest at the knee, but extends far along the thigh. (D) Average principal stretch along the lateral/medial axis for the same participants as in (C). Stretch is consistently larger on the medial compared to the lateral thigh. (E) Stretch on the medial thigh when flexing the knee at different angles. Stretch extends far even at small angles. (F) Principal stretch from distal to proximal along the medial thigh for the same participant as in (E) at the same knee angles. Stretch at the upper thigh grows systematically with knee angle. (G) Local skin area change for the same data as in (F). Away from the knee, skin area does not grow with knee angle, suggesting that the increased principal stretch observed in (F) is compensated for by increased compression in the orthogonal direction. (H) Detailed maps of principal and orthogonal stretch for knee flexion at 70° angle.

stretch induced by joint movements might extend beyond the immediate joint vicinity. Our imaging analysis of skin stretch from the knee to the upper thigh during maximal knee flexion confirmed this hypothesis. As expected, under maximal knee flexion we observed large stretch in excess of 60% directly at the knee joint, but considerable stretch of 10–20% at the upper thigh (figure 2A). The direction of principal stretch was away from the joint, but angling outwards and inwards to the lateral and medial sides of the thigh, respectively (figure 2B). As a consequence the central portion of the thigh displayed stretch in both its principal direction and orthogonally, as the skin was pulled bi-directionally. This pattern persisted across multiple participants: stretch was highest directly at the knee, but persisted above 10% even 15–20 cm away (figure 2C), likely continuing beyond the measured range. However, skin stretch was not solely determined by distance from the knee but also varied across thigh locations, with the lateral side of the knee exhibiting smaller stretch magnitudes than the medial side (figure 2D).

We also tested how skin stretch patterns changed with increasing knee joint angles. For one participant, we imaged the medial thigh during joint angles up to 70°. As expected, principal stretch values increased with joint angle. Notably, the large spatial extent of skin stretch all over the thigh was evident even at the smallest angle tested (20°, figure 2E). While principal stretch increased monotonically with joint angle at all measured distances, stretch values close to the knee were close to saturation at higher angles, while continuing to increase further away (figure 2F). Thus, skin regions away from joints might provide valuable proprioceptive information at higher joint angles that is not available from skin directly at the joint, which might already be maximally extended.

Analysis of the full two-dimensional stretch patterns revealed distinct differences between skin regions near and far from the knee joint. Skin immediately surrounding the joint tended to stretch along both its principal and orthogonal directions, while skin farther away primarily stretched along its principal axis but contracted in the orthogonal direction (see figure 2H for an example). Consequently, while total skin area expanded considerably around the knee, regions distant from the joint exhibited moderate or no change in skin area, even at the largest joint angles tested (figure 2G). These findings impose constraints on whether stretch-sensitive mechanoreceptors relay the relevant signals: receptors near the joint can be sensitive to stretch in any

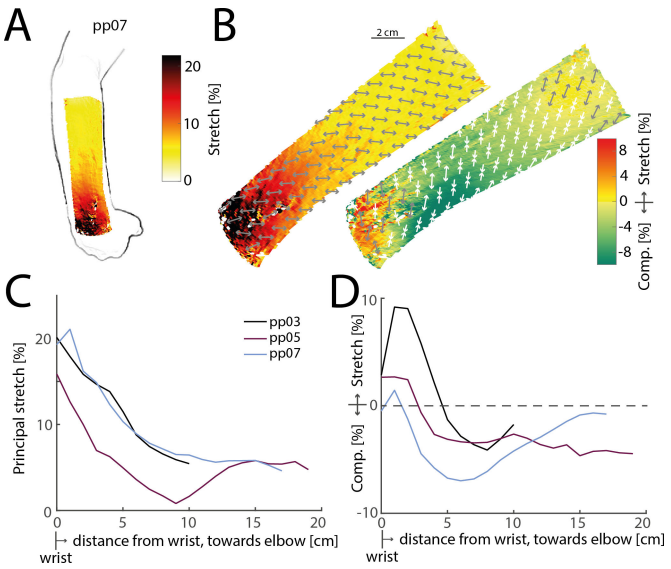


**Figure 3.** Stretch on the forearm due to wrist flexion. (A) Illustration of principal stretch measured on a participant's forearm as the wrist is maximally flexed. (B) Detailed maps of principal (left) and orthogonal (right) stretch for the same participant shown in (A). (C) Average principal stretch at increasing distances from the wrist towards the elbow for three participants. Stretch is highest at the wrist, but extends all the way towards the elbow. (D) Same as in (C), but for stretch orthogonal to the principal direction. The skin is stretched close to the wrist, but compresses in this direction in the middle of the forearm.

direction and reliably convey joint angle information, while receptors elsewhere on the thigh would need to be responsive to stretch along the principal axis specifically, as the skin is only stretched along this axis.

The general trends observed for the knee were mirrored when measuring stretch on the forearm in response to flexion of the wrist (figure 3A,B). Stretch was highest directly at the wrist, but extended onto the forearm and was still measurable even close to the elbow (figure 3C). Again, the skin was stretched in all directions close to the joint, but only stretched along its principal direction further proximally on the forearm, while slightly compressing in the orthogonal direction (figure 3D). As on the knee, the principal direction was not perfectly aligned with the proximal–distal axis along the limb, but instead angled sideways (e.g. medially in the example shown in (figure 3B).

In summary, skin stretch due to joint movements is not limited to skin directly at the joint itself, but extends across the involved limbs: for at least 25 cm beyond the knee on the thigh and 20 cm beyond the wrist on the forearm.

## 2.2. Uniform and large skin stretch on the trunk

Next, we investigated skin stretch in body regions surrounding the trunk, including the neck, back and waist. Unlike hinge joints such as the knee, the neck contains pivot joints, enabling more complex movements. The waist and back are influenced by movements of the spine. Collectively, the trunk region constitutes a large portion of our total body surface, potentially providing strong stretch feedback despite its relatively low innervation density [14].

We found that tilting the head sideways to induce stretch on the neck (figure 4A), curling up in a fetal position to stretch skin on the back (figure 4B), and bending sideways while standing to stretch the side of the waist (figure 4C) consistently induced large, relatively uniform skin stretch that extended beyond the boundaries of tracked regions for all participants. Even the lowest stretch values measured approached 10%, increasing in some cases beyond 50% and averaging 22% on the neck, 23% on the back and 29% on the waist across all participants (figure 4D). Orthogonal to the principal stretch, we measured a slight compression of the skin, averaging between −2% and −3% on all three sites. A notable exception was the skin directly above the spine, which expanded in all directions and exhibited stretch both longitudinally along the spine as well as laterally, with individual vertebrae visible (see figure 4E, right panel).

Stretch on the trunk was spatially uniform. While some subregions exhibited greater stretch than others, the stretch gradient (change in stretch over distance) averaged around 5% $cm^{-1}$, varying across participants and skin sites but never exceeding 10% $cm^{-1}$ (see figure 4F, coloured circles). This suggests that stretch on the trunk decays slowly with distance, affecting a large skin area, similar to our observations on the knee (see figure 4F, grey symbols). Stretch was also uniform in its principal orientation: the average angular standard deviation was 5.7° on the neck, 9.6° on the back and 5.2° on the waist, suggesting that the direction of stretch varied little even across large patches of skin on the trunk (figure 4G). In summary, skin stretch on the trunk is of large magnitude and spatially extensive, fully covering the largest region measured at around 400 $cm^2$ and likely extending further, but relatively uniform in magnitude and orientation.

## 2.3. Spatially complex skin stretch on the face

To explore skin stretch in a region known for its complex movements and lack of traditional proprioceptors, we focused on the cheeks. Facial muscles in this area interact to support facial expressions, speech and mastication, likely resulting in intricate skin deformations. Previous research has suggested that skin stretch serves as a major feedback signal during facial motor

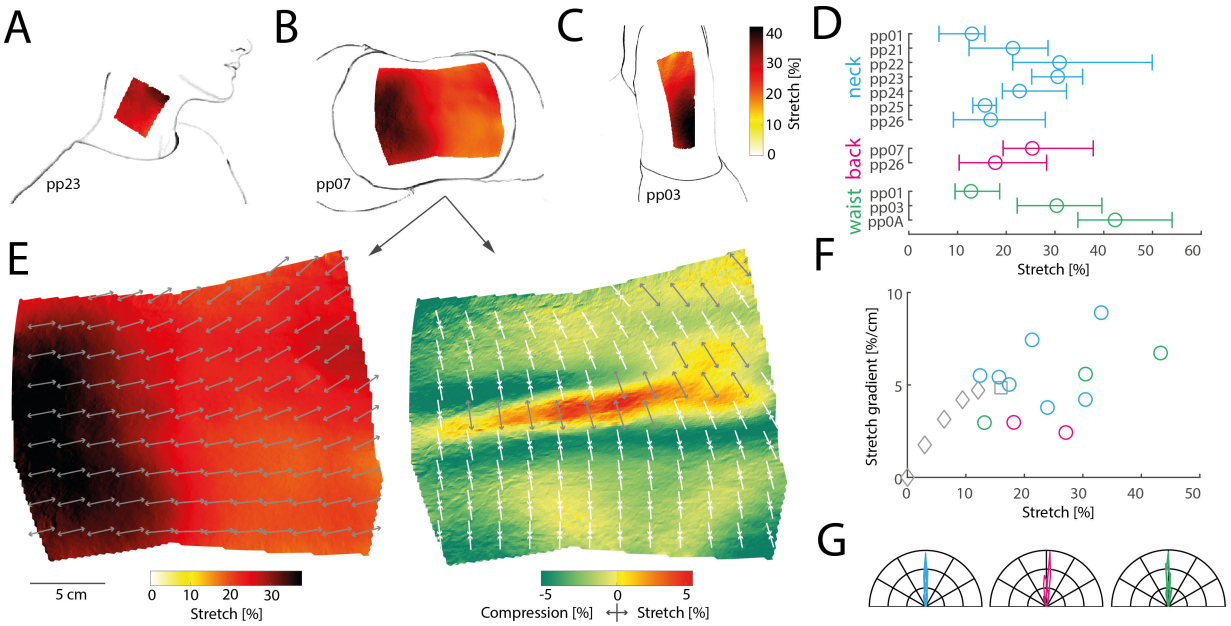


**Figure 4.** Stretch on the body's trunk. Illustrations of principal stretch measured on a participant's neck as the head is bent sideways (A), on the back as the body curls up in the fetal position (B) and on the waist as the body bends sideways (C). (D) Average stretch, and 5th and 95th percentiles for individual participants measured at the neck (blue), back (pink) and waist (green). (E) Detailed principal stretch (left panel) and orthogonal stretch (right panel) on the back for the same participant as in (B). The tracked surface is projected onto the best fitting plane. Arrows indicate the direction of stretch (grey: elongation; white: compression), subsampled and displayed every 2 cm for visibility. The tracked mesh includes 39 139 triangles in total, with an average area of just below 1 $mm^2$ and a total tracked area of 369 $cm^2$ in the unstretched state. (F) Average principal stretch versus stretch gradient for all areas on the trunk (coloured circles) with data from the knee (in grey; diamonds: increasing knee flexion; square: full knee flexion). (G) Polar histograms showing the relative frequency of the principal orientation of stretch across all tracked triangles projected onto the best-fitting two-dimensional plane for the neck, back and waist. Each coloured line denotes a different participant. For each distribution, the average principal stretch orientation has been subtracted from each measured orientation, such that 0° denotes this average, while negative and positive angles show deviations from the average. Stretch is almost entirely uniform for all participants and all skin sites.

control and learning. We measured skin stretch across four distinct facial poses, highlighting the breadth of facial movements: puffing the cheeks, pouting, opening the mouth widely and smiling (see figure 5A for illustrations and refer to Methods §4 for corresponding action units in the Facial Action Coding System).

These poses yielded unique and complex skin stretch patterns compared to other body regions (see figure 5B for example of detailed principal and orthogonal stretch maps). Stretch was generally larger closer to the mouth than laterally on the cheek, which mirrors tactile innervation densities [15]. Thus, when projecting stretch values onto an axis leading from the lower corner of the tracked region (located close to the mouth) to the upper lateral corner (towards the ear), stretch was consistently higher closer to the mouth for all participants and poses (figure 5C). The orientation of stretch also varied more on the cheek area compared to the larger trunk regions, with average angular standard deviations more than twofold those recorded on the trunk (13.0° for puffing, 20.8° for pouting, 17.6° for opening the mouth and 16.1° for smiling, see figure 5D). Furthermore, different poses produced distinct distributions of skin stretch orientations, with opening the mouth eliciting principal orientations nearly perpendicular to those during puffing or pouting (see also figure 5B, grey arrows in top row, for individual examples). This suggests that distinguishing between these poses based on stretch feedback requires considering both stretch magnitude and orientation.

Finally, we noticed that puffing and pouting yielded similar principal stretch patterns: in both instances, stretch was similar in magnitude, spatial arrangement and orientation (see figure 5B, first two panels on top row). However, these two poses resulted in different three-dimensional cheek geometries. While puffing involves outwards bulging of the cheek, pouting leads to a moderate inwards contraction. To successfully disambiguate between these two poses the brain might use information about skin stretch in the direction orthogonal to its principal stretch (see figure 5B, first two panels on bottom row): while orthogonal skin stretch was positive in the puffing condition, signalling an overall expansion of the skin area driven by the outwards bulging of the cheek skin, orthogonal stretch was negative in the pouting condition, signalling a contraction of the skin along this axis (see scatter plot and histograms in figure 5E). This suggests that fully exploiting relevant information in active skin stretch patterns requires mechanoreceptors sensitive to the entire complexity of two-dimensional skin stretch, rather than just coarse measures along a single axis.

In summary, stretch on the face appears more complex compared to other body regions, with most stretch concentrated towards the mouth area.

## 3. Discussion

We measured natural skin stretch induced by different body postures and muscle movements around joints, on multiple trunk regions and on the face. We found widespread and often complex stretch patterns in all regions tested. Around joints, stretch

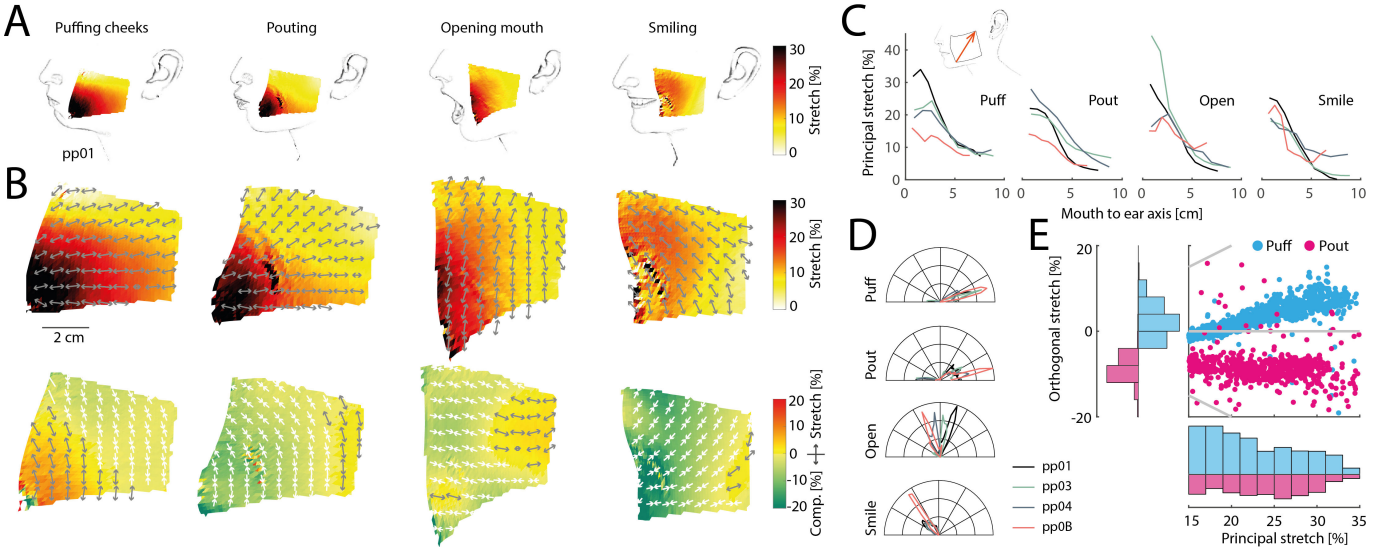


**Figure 5.** Skin stretch on the face during a variety of facial movements. (A) Illustration of poses, tracked area on the cheek and principal stretch for one participant. (B) Detailed maps of principal (top row) and orthogonal stretch (bottom row) for the same participant as in (A). (C) Stretch for all participants projected onto an axis extending from the lower left corner of the tracked area to the upper right (see illustration in inset), therefore roughly extending from the lower mouth in the direction of the ear. Stretch is highest close to the mouth in all four poses and for all participants and decays towards the ear. (D) Polar histograms showing the relative frequency of the principal orientation of stretch across all tracked triangles projected onto the best-fitting two-dimensional plane in the unstretched state. Different panels show different poses. Raw distributions are shown for each pose, so that different angular orientations become evident. (E) Scatter plot (top right) and histograms (left and bottom) of principal and orthogonal stretch for same participants as in (A) during puffing (blue) and pouting (pink). The extent and distribution of the principal stretch is similar in both conditions, while the orthogonal stretch differs, yielding extension in the puffing condition and compression in the pouting condition.

could be measured far from the joint itself, with knee flexion inducing notable skin stretch as far as the upper thigh, tens of centimetres away. On the trunk, bending of the body led to large regions of uniform stretch that often exceeded 20% and more. Finally, different facial poses elicited complex and varying stretch patterns on the cheek, with the highest stretch values measured close to the mouth.

## 3.1. Active stretch induced by body movements

Contact with surfaces often induces shear forces and therefore skin stretch, which can be a salient signal about contact properties. For example, the onset of slip during object grasping induces shear waves on the skin [2,16], which can serve as a rapid signal for making corrective actions. During full slip, skin stretch contributes to signalling the direction of the moving object [17]. Shear forces can also signal the body's movements relative to its surroundings, such as on the foot sole during walking [18] or on the buttocks when seated during acceleration of a vehicle [19].

In contrast to these externally generated skin stretches, here we focused on active skin stretch that is generated by the body itself and that carries information about body conformation. Previous work has mostly focused on skin stretch directly at joints where stretch can be expected to signal joint angle. However, it is likely that relevant stretch signals occur not only in skin directly surrounding the joint, but extend further across the body. For example, flexion of the elbow has previously been shown to stretch skin on the forearm [20] and different ankle postures elicit skin stretch across the foot sole and dorsum, respectively [21]. In the present work, we therefore took a more expansive approach and considered stretch at a multitude of skin regions. Some of the chosen regions have received previous attention: stretch on the back has been investigated using a marker-based set-up [22] as well as optically [23,24], and small patches of skin on the face have previously been imaged for skin stretch [25]. By employing a fully optical method with high spatial resolution, we were able to image skin patches much larger than in previous efforts. As our set-up was optimized for imaging large patches of skin with high resolution, this limited the rate at which images could be acquired. We therefore focused on static postures, ignoring dynamic aspects of the stretch signal, in line with previous research suggesting that skin stretch might be especially important for determining static postures [26]. Choosing a different trade-off between resolution and frame rate or using more advanced cameras would allow recording dynamic information as well (see [23,24], for example). Imaging large body regions with high resolution using a flexible set-up also created some technical challenges, and not all acquired data could be successfully processed (refer to Methods §4 for details). After switching from stamping speckle patterns onto participants to applying tattoo stencils, we noticed a considerable improvement in data quality: the stencils were easier to apply onto curved body regions and less prone to smudging, yielding superior image quality. Body hair was also an issue and future work might consider shaving participants to prevent issues with image registration across different images. Finally, mounting the cameras on a flexible tripod allowed for easy repositioning of the cameras, but required frequent re-calibration of the cameras, and a static approach might be preferable in some set-ups.

### 3.2. Extensive skin stretch across the body

We found that skin stretch often occurs over extensive patches of skin, therefore potentially providing strong and rich feedback. What are the main causes driving widespread stretch? Mechanically, some joints possess skin folds, such as those on the back of the fingers, that support a large movement range as they unfold and absorb the mechanical deformation locally at the joint. A similar principle is at play in elephant trunks, which also display prominent skin folds [27]. However, many human joints do not possess distinctive skin folds and are therefore limited to the skin's general capacity for stretch, which has been found to be anisotropic due to the skin's natural tension [28]. Even in the absence of folds, the skin exhibits furrows and ridges, which mechanically support stretching to some extent [29,30], but might cause more widespread stretch further from the joint to fully support large joint movements. The large extent of stretch along the thigh we observed might partially be caused by this effect. Other body movements, such as bending of the trunk, are not supported by hinge joints, but instead deform the body over a larger region, resulting in extensive skin stretch across large parts of the body. Finally, the underlying geometry of muscles and other body parts themselves can change and deform the skin directly above them, without any direct change in the body's pose. Indeed, tensing of the muscles without any movement of the knee will change the skin conformation of the thigh area especially on the medial side, likely leading to measurable skin stretch patterns without any overt movement of the leg. Thus, skin stretch need not be induced by joint movements *per se*, but could also respond directly to shape changes by the muscles during activation. Overall, the consequence of these disparate mechanisms appears to be widespread stretch patterns.

While the overall stretch patterns were similar across participants, some differences could be observed, for example in the overall amount of stretch present. This diversity might be due to differences in the execution of the poses by individual participants, especially for more complex poses, such as smiling. Some of the observed variability might also reflect differences in the mechanical properties of the skin. An important factor described in the literature is age: older skin is less elastic and shows an increased presence of wrinkles [31,32], both of which will affect whether and how the skin stretches. We included mostly young participants and this study therefore cannot make definitive statements on the effect of age, but the issue warrants further investigation. A decreased capacity for stretch might impoverish the available feedback signal [33], similarly to how touch more generally is affected by age [34].

### 3.3. Stretch as a rich multi-dimensional feedback signal

While skin stretch often exhibited a relatively uniform spatial distribution, particularly on the trunk, its complexity varied across body regions. On the face, for instance, stretch patterns were more intricate, varying spatially in both their principal and orthogonal directions. These findings suggest that skin stretch is not a simple one-dimensional signal along a constant axis defined solely by its magnitude, but rather a complex multidimensional phenomenon: the orientation and magnitude of stretch along both its principal and orthogonal directions all provide valuable and independent cues about changes in body shape. For example, the act of puffing the cheeks results in an expansion of the total skin area of the cheek, as measured by stretch along both the principal and orthogonal axes. An expanding cheek area coupled with the surrounding skin not deforming is only possible if the cheek area deforms in the third dimension, either inwards or outwards. Thus, stretch signals can, in some circumstances, provide hints about the three-dimensional shape of body parts. It is likely that such signals are available to and used by the brain, though perhaps in more basic form, when originating from facial skin: while this region appears mostly devoid of traditional proprioceptors [10], proprioceptive accuracy on both the lips and jaw is high [35]. Local anaesthesia, frequently used in dental surgery, can cause biting of cheeks and other motor control issues [36], possibly due to a lack of tactile feedback. Indeed, skin deformation and its associated cutaneous cues have been implicated in motor learning [12] and speech perception [37,38]. We also possess at least partial awareness of and control over our facial expressions [39], which signal not only the emotional category but also their intensity [40], serve as salient cues to others during social interactions [41], and modulate incoming information from other sensory systems [42]. Finally, tactile perception from inside the mouth, for example during eating, also requires a model of the shape and conformation of the tissues surrounding it [43].

More generally, stretch feedback might support mechanisms that support body perception beyond proprioception, by supplying information about the state of the skin, sometimes called dermatokinesthesis [44], about the size and shape of the body, termed somatoperception [45,46], and perhaps even support representations more classically associated with interoception [47].

### 3.4. Neural mechanisms and perceptual consequences

To effectively utilize stretch signals, especially their complex aspects, the nervous system must first transduce them via mechanoreceptive neurons. Recordings from human primary tactile neurons demonstrate that a significant proportion of tactile neurons innervating the dorsal skin of the hand [48], the thigh [13], the ankle [49] and the face [50] are highly sensitive to skin stretch induced by joint movements, even without additional object contact. Notably, stretch responses were observed in neurons with small receptive fields located distant from the joints, such as responses on the upper thigh during knee flexion [13], suggesting widespread skin sensitivity to local stretch patterns. Indeed, careful experiments involving passive skin stretching revealed that reliable responses in some receptors could be elicited by stretch as low as 1% [9,51], at least an order of magnitude lower than those reported in the present study. This indicates that stretch on all investigated body parts readily exceeds mechanoreceptive thresholds. Slowly adapting type II (SA-II) neurons, thought to innervate Ruffini corpuscles [52], are well-known for their sensitivity to skin stretch, responding to both dynamic and static stretch induced by joint movements

**Table 1.** Full list of participants (pp) and the respective body regions where stretch measurements were taken. A checkmark (✓) indicates data that have been included in the article. Data that have not been included are denoted by different letters; (v): successful data collection and processing, but the targeted body region is not fully visible or the speckle pattern does not extend across the region sufficiently, and therefore, the data were excluded to ensure consistency across participants; (q): data quality were not sufficient and the digital image correlation process failed, for example because of smudging of the ink pattern or the presence of visible body hair in the targeted body region; (c): camera calibration issues prevented three-dimensional reconstruction, for example due to inadvertent movement of the cameras between calibration and data collection. Data for participants from pp06 onwards were collected using the tattoo stencil rather than the stamping method.

| pp → | 0A | 0B | 01 | 02 | 03 | 04 | 05 | 06 | 07 | 21 | 22 | 23 | 24 | 25 | 26 |
|---|---|---|---|---|---|---|---|---|---|---|---|---|---|---|---|
| wrist | | (v) | (q) | (v) | ✓ | (v) | ✓ | (q) | ✓ | | | | | | |
| knee | (q) | | ✓ | (v) | (q) | (v) | ✓ | | | | | ✓ | | | |
| neck | (v) | | ✓ | (v) | (q) | (v) | | | | ✓ | ✓ | ✓ | ✓ | ✓ | ✓ |
| back | (c) | | (c) | (q) | (c) | (c) | | | ✓ | | | | | | ✓ |
| waist | ✓ | | ✓ | (q) | ✓ | (q) | | | | | | | | | |
| face | | ✓ | ✓ | (q) | ✓ | ✓ | | | | | | | | | |

[48]. Indeed, their responses are similar to those of muscle spindle afferents [53]. Some SA-II neurons exhibit tonic activity [54], potentially signalling ongoing skin tension, while also modulating their response rate to subtle skin movements in the absence of an external force [55]. In the hands, SA-II neurons are abundant in the skin at the border of the fingernails, where complex stretch patterns likely occur during fingertip actions [56]. Moreover, stimulation of individual SA-II neurons can often be perceptually detected [57]. These characteristics make SA-II neurons particularly well-suited for signalling precise and ongoing information about the skin's state. However, it is important to note that several other tactile neurons types, including fast adapting ones, also respond to stretch and stretch changes, suggesting a potentially even richer signal.

While not extensively studied, there is evidence that stretch responses are sensitive to the direction of stretch, thereby signalling more intricate aspects of stretch patterns. SA-II neurons have been shown to be sensitive to the direction of stretch, both when the skin is passively stretched [58] and when it is recovering mechanically after a stimulus has been applied [55]. Perceptual experiments have also confirmed our ability to discern the direction of passively applied skin stretch on various body parts [3,59,60]. Moreover, even small movements of the ankle, a multidirectional joint, elicit responses in SA-II and FA-II (Pacinian) neurons across the leg, which as a population convey information about the direction of movement [49], presumably as a consequence of local directional skin stretch. To our knowledge, it is currently unknown whether more complex stretch aspects, such as the stretching or compression of the skin orthogonal to the principal stretch direction, are also reflected in neural responses or perceptually available. Beyond their role in proprioception, skin stretch signals have various perceptual consequences, including changes in thresholds [61,62], two-point discrimination acuity [63], tactile distance estimation [64] and localization [65]. These findings, along with our own, suggest a more profound interconnection between touch and proprioception than previously assumed. Similar to how different touch receptors collaborate to signal relevant tactile features [66,67], information about body state and conformation appears to be distributed across a variety of receptors, encompassing both classical proprioceptive and more traditionally tactile neurons.

# 4. Methods

## 4.1. Participants

Fifteen participants (seven male, seven female and one non-binary) with a mean age of 24.5 (range: 18–41) years and no known allergy against ink were recruited to take part in the study. Not all participants had all skin regions imaged due to time constraints: applying the speckle pattern could be time-consuming (see below) and repositioning the cameras required a new calibration; it was therefore more time efficient to run multiple participants in batches focusing on different subsets of body regions. Additionally, not all trials yielded usable data (see table 1 for the full list of trials and participants included in this report). All participants provided informed consent prior to the start of data collection. The study protocol was approved by the ethical review board of the Department of Psychology at the University of Sheffield (protocol number 053717).

## 4.2. Experimental protocol

At the start of the experimental session, ink-based random speckle patterns were applied to all included skin regions. Speckle patterns were generated in Speckle Generator 1.0.5 Build 209 (Correlated Solutions Inc., Irmo, USA) using a dot diameter of 1.27 mm, a dot density of 65%, and a dot variation of either 75% or 95%. Custom engraved rubber stamps (STAMPIT UK Ltd, London, UK) with these speckle patterns were manufactured in sizes 3.75 by 7.5 cm, 7.5 by 7.5 cm and 14.75 by 14.75 cm, coated in water-based, dermatologically tested ink (Trodat 7011 black, Trodat GmbH, Wels, Austria) and lightly pressed on the participant's skin. Depending on the size of the region tested, multiple stamps would be used. The participant then rested for 15–20 minutes to let the ink dry; in some instances, warm air was directed to the skin through a hairdryer to help the drying process. In a subset of eight participants (see table 1 for full list), speckle patterns were instead printed on A4 tattoo stencil

paper using a thermal printer (LifeBasis, Shenzhen, China). Patches in the required sizes were then cut from these sheets and applied to the relevant skin regions using a small amount of stencil application solution (KMR distributions, Victorville, USA). In these cases, experiments could proceed without the rest period.

After the speckle patterns were applied, participants would sit, stand or lie in front of the camera system, which was focused on the relevant skin region. A series of three to four (multi-camera) images was taken in the relaxed, unstretched pose, which served as the baseline for all stretch calculations. Participants would then assume one or more poses that were presumed to induce skin stretch. For the neck this was bending the head sideways while seated, for the waist bending the body sideways while standing, for the back curling into a fetal position, for the wrist flexing so the palm faced backwards and for the knee flexing to different extents. For the face, four different poses were included: opening the mouth widely (AU27, mouth stretch according to the Facial Action Coding System [68], puffing the cheeks (AU13, cheek puffer), pouting (AU22, lip funneler) and smiling (AU12, lip corner puller). Series of three to four images each were obtained in each pose. For both stretched and unstretched poses, the best (multi-camera) image from each series was selected as a reference image and included in the quantitative analysis presented (refer to Results (§2)). However, stretch values were calculated (see next paragraph) for all suitable images; these are included in the full dataset and were used to test consistency across image acquisitions (see validation section below).

## 4.3. Image acquisition and processing

Images were acquired using a custom built set-up that included four Arducam 64MP autofocus cameras (Arducam Technology Co. Ltd, Hong Kong) for synchronous operation connected via a dedicated UC-512 board (Uctronics, Nanjing, China) to a Raspberry Pi Model 4B (Raspberry Pi Ltd, Cambridge, UK). The board allowed taking 16 MP images (4576 × 3472 pixels each) through all four cameras simultaneously. The cameras were mounted on a tripod using stereoscopic brackets, such that they formed the corners of a rough square of 20 by 20 cm. The set-up was positioned at roughly 30 cm distance from the targeted skin region and supported by LED lights to provide illumination. The cameras were calibrated in pairs using standard stereo checkerboard images, resulting in reprojection errors of 3.3 pixels on average (across 17 individual camera calibrations), with a single pixel located centrally in the image covering a region of roughly 0.1 by 0.1 mm in size.

## 4.4. Calculation of skin stretch measures

Images were processed using the open DuoDIC [69] package in Matlab (Mathworks Inc., Natick, USA). In short, using digital image correlation (DIC), the software matches small speckle patches both across cameras and across different poses by cross-correlating the images obtained from different cameras and at different poses under different image transformations. We typically used a patch radius of 60 pixels and a spacing of 10 pixels, yielding several thousand tracked points across the full skin patch at sub-millimetre resolution. In some instances, this process failed as reliable image correlations could not be found by the algorithm. This could happen because of deficiencies in the ink pattern (e.g. smudged ink), which prevented matching image patches. In other participants, body hair, for example on the arms or the face, impaired the correlation method, and shaving the targeted skin region might be required for robust tracking in such cases. Nineteen individual skin regions were ultimately successfully processed using DIC and further analysed (see table 1 for the full list). First, by considering corresponding points in the images across multiple cameras, they were projected into three-dimensional space and triangulated, yielding a three-dimensional surface. Tracked skin patches contained on average 9327 triangular faces (range: 2142–39 139), with an average size of 0.9 $mm^2$ (0.5–2.4 $mm^2$) each, covering an average skin area of 102.4 $cm^2$, which could vary considerably depending on the region (21.2–397.5 $cm^2$ from the face to the back, respectively). Next, by considering the difference in three-dimensional shape between the relaxed pose and the target pose, the resulting stretch and compression along the two-dimensional surface was calculated for each triangle that made up the surface. Specifically, we used principal Lagrangian strains, which decomposes the deformation into two values: the stretch along the direction where it is maximal (principal stretch) and the stretch or compression along the direction orthogonal to this principal direction.

For visualizations, we calculated the best-fitting plane for each skin patch and projected the surface on it, using custom code and the matGEOM Matlab package [70]. Next, we resampled stretch magnitudes and orientations on a grid with 1 mm resolution. We found that the vast majority of total summed strain for each body site was constrained to this plane (97% on average, with a minimum of 90%), and the resulting two-dimensional representations therefore capture the skin deformations well.

## 4.5. Validation of method and accuracy

To test the accuracy with which our set-up could determine stretch under different viewing conditions, we systematically deformed the speckle patterns in Adobe Illustrator (Adobe Inc., San Jose, USA) and imaged printouts of the patterns under different viewing angles. We then used the analysis pipeline described above to calculate the resulting deformations and stretch patterns and compared them against the ground truth. We found excellent three-dimensional reconstruction accuracy with errors for individual tracked points of 0.2 mm on average for different viewing angles and under stretched conditions. Imaging the same baseline speckle pattern multiple times, either in the same view or under a changed viewing angle, should yield stretch values close to zero. Indeed, we found average absolute errors of 0.3% when the speckle patterns position was unchanged and 0.4% when the viewing angle was adjusted, demonstrating that inherent noise was low. When uni-axial uniform

stretch of 33% was applied to the speckle pattern, the resulting stretch values differed on average by 0.9% in the same pose and 0.3% under a different viewing angle along the principal direction, and by 0.4% and 0.3%, respectively, in the orthogonal direction. Thus, errors were on average one to two orders of magnitude lower than the main effects reported in this study.

We also compared stretch values across multiple image acquisitions in the same pose. First, we tested how well stretch patterns agreed when images were taken in quick succession. We found that for the back (the largest region imaged), stretch values were on average highly correlated across multiple acquisitions, both along the principal stretch direction ($r = 0.99$) and the orthogonal direction ($r = 0.95$). Moreover, the standard deviation of average principal stretch values across multiple images was small (< 0.8%). Next, we tested the consistency of the stretch patterns when the same pose was repeatedly attained from the unstretched baseline. We used data from the neck for a subset of participants (pp21–pp26), which had been asked to bend their neck four separate times. We again found that stretch values were highly correlated along the principal ($r = 0.89$) and orthogonal axes ($r = 0.79$) and the standard deviation of the average principal stretch was low (< 3.2%). However, overall variability was higher, likely caused by slight differences in the final pose attained.

Ethics. The study protocol was approved by the ethical review board of the Department of Psychology at the University of Sheffield (protocol number 053717). Participants provided written consent to take part in the study and for their images to be used.

Data accessibility. All processed DIC data and anonymized reference images are available on Zenodo [71].

Declaration of AI use. We have not used AI-assisted technologies in creating this article.

Authors' contributions. M.R.: conceptualization, data curation, investigation, methodology, project administration, visualization, writing—review and editing; L.D.C.: conceptualization, investigation, methodology, writing—review and editing; H.P.S.: conceptualization, data curation, funding acquisition, supervision, visualization, writing—original draft.

All authors gave final approval for publication and agreed to be held accountable for the work performed therein.

Funding. MR was supported, in part, by a Sheffield Undergraduate Research Experience (SURE) fellowship. LDC was supported by a studentship from the MRC Discovery Medicine North (DiMeN) Doctoral Training Partnership (MR/N013840/1). HPS was supported by the Leverhulme Trust under Research Project Grant RPG-2022-031.

Acknowledgements. We would like to thank Rory Holmes for help in developing the image acquisition software, Anika Kao, Greg Gerling, Sarah Crossland and Claire Brockett for helpful suggestions improving the experimental set-up, Chaona Chen for sharing knowledge about facial expressions, and all participants for supporting these experiments.

# References

1. Delhaye B, Barrea A, Edin BB, Lefèvre P, Thonnard JL. 2016 Surface strain measurements of fingertip skin under shearing. *J. R. Soc. Interface* **13**, 20150874–20150874. (doi:10.1098/rsif.2015.0874)
2. Delhaye BP, Jarocka E, Barrea A, Thonnard JL, Edin B, Lefèvre P. 2021 High-resolution imaging of skin deformation shows that afferents from human fingertips signal slip onset. *Elife* **10**. (doi:10.7554/eLife.64679)
3. Olausson H, Hamadeh I, Pakdel P, Norrsell U. 1998 Remarkable capacity for perception of the direction of skin pull in man. *Brain Res*. **808**, 120–123. (doi:10.1016/s0006-8993(98)00838-5)
4. Edin BB, Johansson N. 1995 Skin strain patterns provide kinaesthetic information to the human central nervous system. *J Physiol* **487**, 243–251. (doi:10.1113/jphysiol.1995.sp020875)
5. Collins DF, Prochazka A. 1996 Movement illusions evoked by ensemble cutaneous input from the dorsum of the human hand. *J Physiol* **496**, 857–871. (doi:10.1113/jphysiol.1996.sp021733)
6. Collins DF, Refshauge KM, Todd G, Gandevia SC. 2005 Cutaneous receptors contribute to kinesthesia at the index finger, elbow, and knee. *J. Neurophysiol*. **94**, 1699–1706. (doi:10.1152/jn.00191.2005)
7. Kuling IA, Brenner E, Smeets JBJ. 2016 Proprioceptive localization of the hand changes when skin stretch around the elbow is manipulated. *Front. Psychol*. **7**, 1620. (doi:10.3389/fpsyg.2016.01620)
8. Macefield VG. 2021 The roles of mechanoreceptors in muscle and skin in human proprioception. *Curr Opin Physiol* **21**, 48–56. (doi:10.1016/j.cophys.2021.03.003)
9. Edin BB. 1992 Quantitative analysis of static strain sensitivity in human mechanoreceptors from hairy skin. *J. Neurophysiol*. **67**, 1105–1113. (doi:10.1152/jn.1992.67.5.1105)
10. Cobo JL, Abbate F, de Vicente JC, Cobo J, Vega JA. 2017 Searching for proprioceptors in human facial muscles. *Neurosci. Lett*. **640**, 1–5. (doi:10.1016/j.neulet.2017.01.016)
11. Staloff IA, Rafailovitch M. 2008 Measurement of skin stretch using digital image speckle correlation. *Ski. Res. Technol*. **14**, 298–303. (doi:10.1111/j.1600-0846.2008.00294.x)
12. Ito T, Ostry DJ. 2010 Somatosensory contribution to motor learning due to facial skin deformation. *J. Neurophysiol*. **104**, 1230–1238. (doi:10.1152/jn.00199.2010)
13. Edin B. 2001 Cutaneous afferents provide information about knee joint movements in humans. *J Physiol* **531**, 289–297. (doi:10.1111/j.1469-7793.2001.0289j.x)
14. Corniani G, Saal HP. 2020 Tactile innervation densities across the whole body. *J. Neurophysiol*. **124**, 1229–1240. (doi:10.1152/jn.00313.2020)
15. Johansson RS, Trulsson M, Olsson KA, Westberg KG. 1988 Mechanoreceptor activity from the human face and oral mucosa. *Exp. Brain Res*. **72**, 204–208. (doi:10.1007/BF00248518)
16. Delhaye BP, Schiltz F, Crevecoeur F, Thonnard JL, Lefèvre P. 2024 Fast grip force adaptation to friction relies on localized fingerpad strains. *Sci. Adv*. **10**, eadh9344. (doi:10.1126/sciadv.adh9344)
17. Seizova-Cajic T, Karlsson K, Bergstrom S, McIntyre S, Birznieks I. 2014 Lateral skin stretch influences direction judgments of motion across the skin. In *Haptics: neuroscience, devices, modeling, and applications, lecture notes in computer science*, pp. 425–431. Berlin, Germany: Springer. (doi:10.1007/978-3-662-44193-0_53)
18. Crossland SR, Siddle HJ, Culmer P, Brockett CL. 2022 A plantar surface shear strain methodology utilising digital image correlation. *J. Mech. Behav. Biomed. Mater*. **136**, 105482. (doi:10.1016/j.jmbbm.2022.105482)
19. Horie A, Nagano H, Konyo M, Tadokoro S. 2018 Buttock skin stretch: inducing shear force perception and acceleration illusion on self-motion perception. In *Haptics: science, technology, and applications*. Cham, Switzerland: Springer International Publishing.
20. Maiti R *et al*. 2016 *In vivo* measurement of skin surface strain and sub-surface layer deformation induced by natural tissue stretching. *J. Mech. Behav. Biomed. Mater*. **62**, 556–569. (doi:10.1016/j.jmbbm.2016.05.035)

21. Smith SGVS, Yokich MK, Beaudette SM, Brown SHM, Bent LR. 2019 Effects of foot position on skin structural deformation. *J. Mech. Behav. Biomed. Mater*. **95**, 240–248. (doi:10.1016/j.jmbbm.2019.04.012)
22. Beaudette SM, Zwambag DP, Bent LR, Brown SHM. 2017 Spine postural change elicits localized skin structural deformation of the trunk dorsum *in vivo*. *J. Mech. Behav. Biomed. Mater*. **67**, 31–39. (doi:10.1016/j.jmbbm.2016.11.025)
23. Kao AR, Xu C, Gerling GJ. 2022 Using digital image correlation to quantify skin deformation with Von Frey monofilaments. *IEEE Trans. Haptics* **15**, 26–31. (doi:10.1109/TOH.2021.3138350)
24. Kao AR, Landsman ZT, Gerling GJ, Loghmani MT. 2023 Optical measurements of the skin surface to infer bilateral distinctions in myofascial tissue stiffness. *World Haptics Conf* **2023**, 244–251. (doi:10.1109/whc56415.2023.10224420)
25. Staloff IA, Guan E, Katz S, Rafailovitch M, Sokolov A, Sokolov S. 2008 An *in vivo* study of the mechanical properties of facial skin and influence of aging using digital image speckle correlation. *Ski. Res. Technol*. **14**, 127–134. (doi:10.1111/j.1600-0846.2007.00266.x)
26. Cordo PJ, Horn JL, Künster D, Cherry A, Bratt A, Gurfinkel V. 2011 Contributions of skin and muscle afferent input to movement sense in the human hand. *J. Neurophysiol*. **105**, 1879–1888. (doi:10.1152/jn.00201.2010)
27. Schulz AK *et al*. 2022 Skin wrinkles and folds enable asymmetric stretch in the elephant trunk. *Proc. Natl Acad. Sci. USA*. **119**, e2122563119. (doi:10.1073/pnas.2122563119)
28. Ní Annaidh A, Bruyère K, Destrade M, Gilchrist MD, Otténio M. 2012 Characterization of the anisotropic mechanical properties of excised human skin. *J. Mech. Behav. Biomed. Mater*. **5**, 139–148. (doi:10.1016/j.jmbbm.2011.08.016)
29. Leyva-Mendivil MF, Page A, Bressloff NW, Limbert G. 2015 A mechanistic insight into the mechanical role of the stratum corneum during stretching and compression of the skin. *J. Mech. Behav. Biomed. Mater*. **49**, 197–219. (doi:10.1016/j.jmbbm.2015.05.010)
30. Corniani G, Lee ZS, Carré MJ, Lewis R, Delhaye BP, Saal HP. 2023 Sub-surface deformation of individual fingerprint ridges during tactile interactions. *Neuroscience* 2023.07.02.547395. (doi:10.1101/2023.07.02.547395)
31. Daly CH, Odland GF. 1979 Age-related changes in the mechanical properties of human skin. *J. Investig. Dermatol*. **73**, 84–87. (doi:10.1111/1523-1747.ep12532770)
32. Pawlaczyk M, Lelonkiewicz M, Wieczorowski M. 2013 Age-dependent biomechanical properties of the skin. *Postepy Dermatol. I Alergol*. **30**, 302–306. (doi:10.5114/pdia.2013.38359)
33. Deflorio D, Di Luca M, Wing AM. 2022 Skin properties and afferent density in the deterioration of tactile spatial acuity with age. *J Physiol* **601**, 517–533. (doi:10.1113/JP283174)
34. McIntyre S, Nagi SS, McGlone F, Olausson H. 2021 The effects of ageing on tactile function in humans. *Neuroscience* **464**, 53–58. (doi:10.1016/j.neuroscience.2021.02.015)
35. Frayne E, Coulson S, Adams R, Croxson G, Waddington G. 2016 Proprioceptive ability at the lips and jaw measured using the same psychophysical discrimination task. *Exp. Brain Res*. **234**, 1679–1687. (doi:10.1007/s00221-016-4573-0)
36. Hersh EV, Moore PA, Papas AS, Goodson JM, Navalta LA, Rogy S, Rutherford B, Yagiela JA, Soft Tissue Anesthesia Recovery Group. 2008 Reversal of soft-tissue local anesthesia with phentolamine mesylate in adolescents and adults. *J. Am. Dent. Assoc.***139**, 1080–1093. (doi:10.14219/jada.archive.2008.0311)
37. Ito T, Tiede M, Ostry DJ. 2009 Somatosensory function in speech perception. *Proc. Natl Acad. Sci. USA*. **106**, 1245–1248. (doi:10.1073/pnas.0810063106)
38. Franken MK, Liu BC, Ostry DJ. 2022 Towards a somatosensory theory of speech perception. *J. Neurophysiol*. **128**, 1683–1695. (doi:10.1152/jn.00381.2022)
39. Ciston AB, Forster C, Brick TR, Kühn S, Verrel J, Filevich E. 2022 Do I look like I'm sure?: Partial metacognitive access to the low-level aspects of one's own facial expressions. *Cognition* **225**, 105155. (doi:10.1016/j.cognition.2022.105155)
40. Chen C, Messinger DS, Chen C, Yan H, Duan Y, Ince RAA, Garrod OGB, Schyns PG, Jack RE. 2024 Cultural facial expressions dynamically convey emotion category and intensity information. *Curr. Biol*. **34**, 213–223. (doi:10.1016/j.cub.2023.12.001)
41. Chen C, Garrod OGB, Schyns PG, Jack RE. 2020 Dynamic Face Movement Texture Enhances the Perceived Realism of Facial Expressions of Emotion. In *Proc. of the 20th ACM Int. Conf. on Intelligent Virtual Agents*, Virtual Event Scotland UK. New York, NY: ACM. (doi:10.1145/3383652.3423912). https://dl.acm.org/doi/proceedings/10.1145/3383652.
42. Susskind JM, Lee DH, Cusi A, Feiman R, Grabski W, Anderson AK. 2008 Expressing fear enhances sensory acquisition. *Nat. Neurosci*. **11**, 843–850. (doi:10.1038/nn.2138)
43. Haggard P, Boer L. 2014 Oral somatosensory awareness. *Neurosci. Biobehav. Rev*. **47**, 469–484. (doi:10.1016/j.neubiorev.2014.09.015)
44. Halpern L. 1946 Dermatokinaesthesis. *Eur. Neurol*. **112**, 348–354. (doi:10.1159/000148320)
45. Longo MR, Azañón E, Haggard P. 2010 More than skin deep: body representation beyond primary somatosensory cortex. *Neuropsychologia* **48**, 655–668. (doi:10.1016/j.neuropsychologia.2009.08.022)
46. Longo MR, Haggard P. 2012 A 2.5-D representation of the human hand. *J. Exp. Psychol. Hum. Percept. Perform*. **38**, 9–13. (doi:10.1037/a0025428)
47. Crucianelli L, Ehrsson HH. 2023 The role of the skin in interoception: a neglected organ? *Perspect. Psychol. Sci*. **18**, 224–238. (doi:10.1177/17456916221094509)
48. Edin BB, Abbs JH. 1991 Finger movement responses of cutaneous mechanoreceptors in the dorsal skin of the human hand. *J. Neurophysiol*. **65**, 657–670. (doi:10.1152/jn.1991.65.3.657)
49. Aimonetti JM, Hospod V, Roll JP, Ribot-Ciscar E. 2007 Cutaneous afferents provide a neuronal population vector that encodes the orientation of human ankle movements. *J Physiol* **580**, 649–658. (doi:10.1113/jphysiol.2006.123075)
50. Johansson RS, Trulsson M, Olsson KA, Abbs JH. 1988 Mechanoreceptive afferent activity in the infraorbital nerve in man during speech and chewing movements. *Exp. Brain Res*. **72**, 209–214. (doi:10.1007/BF00248519)
51. Edin BB. 2004 Quantitative analyses of dynamic strain sensitivity in human skin mechanoreceptors. *J. Neurophysiol*. **92**, 3233–3243. (doi:10.1152/jn.00628.2004)
52. Halata Z. 1988 Ruffini corpuscle—a stretch receptor in the connective tissue of the skin and locomotion apparatus. *Prog. Brain Res*. **74**, 221–229. (doi:10.1016/s0079-6123(08)63017-4)
53. Grill SE, Hallett M. 1995 Velocity sensitivity of human muscle spindle afferents and slowly adapting type II cutaneous mechanoreceptors. *J Physiol* **489**, 593–602. (doi:10.1113/jphysiol.1995.sp021075)
54. Chambers MR, Andres KH, von Duering M, Iggo A. 1972 The structure and function of the slowly adapting type II mechanoreceptor in hairy skin. *Q. J. Exp. Physiol. Cogn. Med. Sci*. **57**, 417–445. (doi:10.1113/expphysiol.1972.sp002177)
55. Saal HP, Birznieks I, Johansson RS. 2023 Memory at your fingertips: how viscoelasticity affects tactile neuron signaling. *BioRxiv* 2023.05.15.540820.
56. Birznieks I, Macefield VG, Westling G, Johansson RS. 2009 Slowly adapting mechanoreceptors in the borders of the human fingernail encode fingertip forces. *J. Neurosci*. **29**. (doi:10.1523/JNEUROSCI.0143-09.2009)
57. Watkins RH, Amante M, Wasling HB, Wessberg J, Ackerley R. 2022 Slowly-adapting type II afferents contribute to conscious touch sensation in humans: evidence from single unit intraneural microstimulation. *J Physiol* **600**, 2939–2952. (doi:10.1113/JP282873)
58. Grigg P. 1996 Stretch sensitivity of mechanoreceptor neurons in rat hairy skin. *J. Neurophysiol*. **76**, 2886–2895. (doi:10.1152/jn.1996.76.5.2886)

59. Gleeson BT, Horschel SK, Provancher WR. 2009 Communication of direction through lateral skin stretch at the fingertip. In *World Haptics 2009—Third Joint EuroHaptics Conf. and Symp. on Haptic Interfaces for Virtual Environment and Teleoperator Systems*, Salt Lake City, UT, pp. 172–177. Piscataway, NJ: IEEE. (doi:10.1109/WHC.2009.4810804)
60. Chen D, Anderson I, Walker C, Besier T. 2016 Lower extremity lateral skin stretch perception for haptic feedback. *IEEE Trans. Haptics* **9**, 62–68. (doi:10.1109/TOH.2016.2516012)
61. Beaudette SM, Smith SGVS, Bent LR, Brown SHM. 2017 Spine posture influences tactile perceptual sensitivity of the trunk dorsum. *Ann. Biomed. Eng*. **45**, 2804–2812. (doi:10.1007/s10439-017-1924-3)
62. Smith SGVS, Yokich MK, Beaudette SM, Brown SHM, Bent LR. 2021 Cutaneous sensitivity across regions of the foot sole and dorsum are influenced by foot posture. *Front. Bioeng. Biotechnol*. **9**, 744307. (doi:10.3389/fbioe.2021.744307)
63. Cody FWJ, Idrees R, Spilioti DX, Poliakoff E. 2010 Tactile spatial acuity is reduced by skin stretch at the human wrist. *Neurosci. Lett*. **484**, 71–75. (doi:10.1016/j.neulet.2010.08.022)
64. Mainka T, Ganos C, Longo MR. 2023 Skin stretch modulates tactile distance perception without central correction mechanisms. *J. Exp. Psychol. Hum. Percept. Perform*. **49**, 226–235. (doi:10.1037/xhp0001063)
65. Kang W, Longo MR. 2023 Tactile localization on stretched skin. *J. Exp. Psychol. Hum. Percept. Perform*. **49**, 1175–1179. (doi:10.1037/xhp0001142)
66. Saal HP, Bensmaia SJ. 2014 Touch is a team effort: interplay of submodalities in cutaneous sensibility. *Trends Neurosci*. **37**, 689–697. (doi:10.1016/j.tins.2014.08.012)
67. Corniani G, Casal MA, Panzeri S, Saal HP. 2022 Population coding strategies in human tactile afferents. *PLoS Comput. Biol*. **18**, e1010763. (doi:10.1371/journal.pcbi.1010763)
68. Ekman P, Friesen WV. 1976 Measuring facial movement. *J. Nonverbal Behav*. **1**, 56–75. (doi:10.1007/BF01115465)
69. Solav D, Silverstein A. 2022 DuoDIC: 3D Digital Image Correlation in MATLAB. *JOSS* **7**, 4279. (doi:10.21105/joss.04279)
70. Legland D. 2025 MatGeom: a toolbox for geometry processing with MATLAB. *SoftwareX* **29**, 101984. (doi:10.1016/j.softx.2024.101984)
71. Rupani M, Cleland L, Saal H. 2024 Local postural changes elicit extensive and diverse skin stretch around joints, on the trunk, and the face. *Zenodo* (doi:10.5281/zenodo.13939433)